Spontaneous Action Potentials Initiate Rhythmic Intercellular Calcium Waves in Immortalized Hypothalamic (GT1–1) Neurons

JAMES L. COSTANTIN AND ANDREW C. CHARLES
Department of Neurology, UCLA School of Medicine, Los Angeles, California 90095-1769

Costantin, James L. and Andrew C. Charles. Spontaneous action potentials initiate rhythmic intercellular calcium waves in immortalized hypothalamic (GT1–1) neurons. *J. Neurophysiol.* 82: 429–435, 1999. GT1–1 cells exhibit spontaneous action potentials and transient increases in intracellular calcium concentration ($[Ca^{2+}]_i$) that occur in individual cells and as spatially propagated intercellular Ca^{2+} waves. In this study, simultaneous cell-attached patch-clamp recording of action currents (indicative of action potentials) and fluorescence imaging of $[Ca^{2+}]_i$ revealed that Ca^{2+} transients in GT1–1 cells were preceded by a single action current or a burst of action currents. Action currents preceded Ca^{2+} transients in a similar pattern regardless of whether the Ca^{2+} transients were limited to the individual cell or occurred as part of an intercellular Ca^{2+} wave. Both the action currents and Ca^{2+} transients were abolished by 1 μM tetrodotoxin. Removal of extracellular Ca^{2+} abolished all spontaneous Ca^{2+} transients without inhibiting the firing of action currents. Nimodipine, which blocks L-type Ca^{2+} currents in GT1–1 cells, also abolished all spontaneous Ca^{2+} signaling. Delivery of small voltage steps to the patch pipette in the cell-attached configuration elicited action currents the latency to firing of which decreased with increasing amplitude of the voltage step. These results indicate that spontaneous intercellular Ca^{2+} waves are generated by a propagated depolarization, the firing of action potentials in individual cells, and the resulting influx of Ca^{2+} through L-type Ca^{2+} channels. These patterns of spontaneous activity may be important in driving the pulsatile release of GnRH from networks of cells.

INTRODUCTION

Rhythmic release of hormones is a fundamental property of the endocrine reproductive axis. The rhythmic, pulsatile release of luteinizing hormone (LH) from the anterior pituitary is driven by the pulsatile release of gonadotropin releasing hormone (GnRH) from neurons located in the hypothalamus (Clarke and Cummins 1982; Knobil 1980). Multiple lines of evidence indicate that the ability to release GnRH in a pulsatile fashion is an intrinsic property of GnRH neurons. Hypothalamic explants and primary cell cultures derived from the hypothalamus have been shown to release GnRH in a pulsatile manner (Bourguignon et al. 1993; Krsmanovic et al. 1992). However, the mechanisms of GnRH release by individual cells and the processes by which the activity of a network of neurons is coordinated to produce a pulsatile pattern of GnRH release remain poorly understood.

GnRH neurons in vivo exhibit changes in spontaneous electrophysiological activity that are correlated with pulsatile hormone release. LH pulses have been correlated with increases in multiunit activity (MUA volleys) recorded in the medial basal hypothalamus of the rat (Kawakami et al. 1982), rhesus monkey (Knobil 1988; Wilson et al. 1984), and goat (Mori et al. 1991). Examination of the single unit component of the MUA volley suggests that the increased activity is a result of an increase in the firing rate of individual neurons rather than the recruitment of new bursting neurons (Cardenas et al. 1993).

The development of immortalized cell lines of GnRH releasing neurons has provided the opportunity to study the electrophysiological activity of GnRH neurons in a reliable and accessible in vitro preparation. The GT1 cell lines are immortalized GnRH neuronal lines derived by genetically targeted tumorigenesis in transgenic mice (Mellon et al. 1990). GT1 cells are highly differentiated neurons both morphologically and functionally (Wetsel 1995), and they release GnRH in a pulsatile manner with a 25- to 35-min interpulse interval (Martinez de la Escalera et al. 1992; Wetsel et al. 1992). Multiple clones of the GT1 line were established, including the GT1–1 and GT1–7 lines. Both GT1–1 and GT1–7 cells exhibit spontaneous action potentials and Ca^{2+} transients in individual cells (Charles and Hales 1995; Hales et al. 1994). In addition, the GT1–1 line (but not the GT1–7 line) shows waves of increased $[Ca^{2+}]_i$ that are propagated across fields of hundreds of cells (Charles et al. 1996). The existence of intercellular Ca^{2+} waves in GT1–1 cells, the property of dye coupling between these cells, and the levels of expression of the gap junction protein connexin26 suggest that the Ca^{2+} waves are propagated primarily via gap junctions (Charles et al. 1996).

To further investigate the mechanisms of intrinsic electrophysiological activity of GT1–1 cells and the processes by which this activity is coordinated in networks of cells, we have examined the spontaneous activity of GT1–1 cells with simultaneous cell-attached patch-clamp recording of a single cell and video imaging of $[Ca^{2+}]_i$ from the entire field of cells containing the patched cell.

METHODS

Electrophysiological recording

CELL-ATTACHED PATCH-CLAMP RECORDING. Action currents were measured in the cell-attached configuration (Hamill et al. 1981) as a capacitive current that charges the membrane (Charles and Hales 1995; Fenwick et al. 1982; Peters et al. 1989). The advantage of measuring action currents in the cell-attached configuration, as compared with whole cell recording of action potentials, is that the intracellular contents of a cell are not disturbed while action currents are monitored. The records are displayed as they appeared on the oscilloscope, i.e., patch outward ionic current in the cell-attached configuration is plotted as a negative (downward) current. The patch

The costs of publication of this article were defrayed in part by the payment of page charges. The article must therefore be hereby marked "*advertisement*" in accordance with 18 U.S.C. Section 1734 solely to indicate this fact.

is voltage clamped to 0 mV relative to the bath. The capacitive current that is measured when the cell fires an action potential appears as a brief spike in the downward direction. The bath and pipette solution consisted of (in mM) 137 NaCl, 2.8 KCl, 2.0 $MgCl_2$, 1.0 $CaCl_2$, 10 glucose, and 10 HEPES (pH 7.2 with NaOH); nominally Ca^{2+}-free solution was the same except 1.0 mM $CaCl_2$ was not added. Axon instruments software (Axoscope and pClamp 7) and a Digidata 1200 A/D board were used to record the action currents onto a Pentium PC.

WHOLE CELL PATCH-CLAMP RECORDING. Ca^{2+} channels were recorded using a bath solution containing (in mM): 115 NaCl, 5.4 CsCl, 10.8 $BaCl_2$, 1.0 $MgCl_2$, 10 glucose, and 10 HEPES plus 0.5 μM TTX (pH 7.2 adjusted with NaOH), and a pipette solution containing (in mM): 130 CsCl, 10 EGTA, 3 MgATP, and 10 HEPES (pH 7.2 adjusted with CsOH). The leak subtraction voltage protocol used was P/N = −4 (Bezanilla and Armstrong 1977).

VIDEO FLUORESCENCE IMAGING. Changes in $[Ca^{2+}]_i$ were measured after loading the cells in the bath solution with 5 μM fura2 (Calbiochem) for 30–40 min. We measured $[Ca^{2+}]_i$ with a fluorescence imaging system and analysis methods described previously (Charles et al. 1991). Some sequences of fura2 fluorescence were recorded to videotape and subsequently digitized using the Axon Imaging Workbench software and Digidata 2000 A/D board (Axon Instruments). The change in fura2 fluorescence measured with 380-nm excitation (ΔF) is shown in pixel intensity values (0–255 scale). The bath solution used for video fluorescence experiments was the same as that used for cell-attached patch-clamp recording.

CORRELATING VIDEO IMAGING WITH ELECTROPHYSIOLOGY. Synchronization of the cell-attached electrophysiological experiments with the fluorescence microscopy was achieved by simultaneously placing an audio tag on the videotape and a digital tag on the Axoscope file. The tags were aligned with respect to time by the frame number on the video tape and by their position on the Axoscope file. A single-frame animation video cassette recorder (Sanyo GVR-S950) was used. The Society of Motion Picture and Television Engineers (SMPTE) method of identifying individual frames was used. The SMPTE time code was ''striped'' onto audio channel 2 using the VCR and the audio tag on channel 1 was assigned a frame number. Thus individual tags on the Axoscope file could be correlated with a frame number on the videotape.

CELL CULTURE. GT1–1 cells were a generous gift of Dr. Richard Weiner. Cells were maintained in culture in DMEM/F12 media (Mediatech, Cat No. 10–092) supplemented with 5% fetal bovine serum, 5% horse serum, 100 IU/ml penicillin and 100 μg/ml streptomycin in 25^2 cm flasks. Cells were grown to ~60–80% confluency and then passaged or transferred onto poly-D-lysine-coated glass coverslips, on which they were grown for 3–10 days to a confluence of ~60–80% before experimentation.

RESULTS

Simultaneous measurements of electrical activity and $[Ca^{2+}]_i$ in GT1–1 cells revealed that each increase in $[Ca^{2+}]_i$ was preceded by a single action current or a burst of action currents (n = 6 different coverslips). The patterns of action currents observed with simultaneous measurements of $[Ca^{2+}]_i$ were consistent with independent measurements of action currents (n = 42) and $[Ca^{2+}]_i$ (n = 33). A typical example of a continuous recording of action currents (spikes) measured using the cell-attached patch-clamp technique (Fig. 1*A*) is shown with the corresponding $[Ca^{2+}]_i$ measurements obtained using fluorescence microscopy (Fig. 1*B*). The Ca^{2+} oscillations followed the action currents after a variable latency. A small percentage of action currents were not associated with an increase in $[Ca^{2+}]_i$ (Fig. 1*Ae*). There was considerable variability in the duration of action current bursts and in the number of spikes per burst (Fig. 1*C*). In most cases, subsequent bursts of action currents occurred only after $[Ca^{2+}]_i$ had recovered fully from the increase associated with the previous burst.

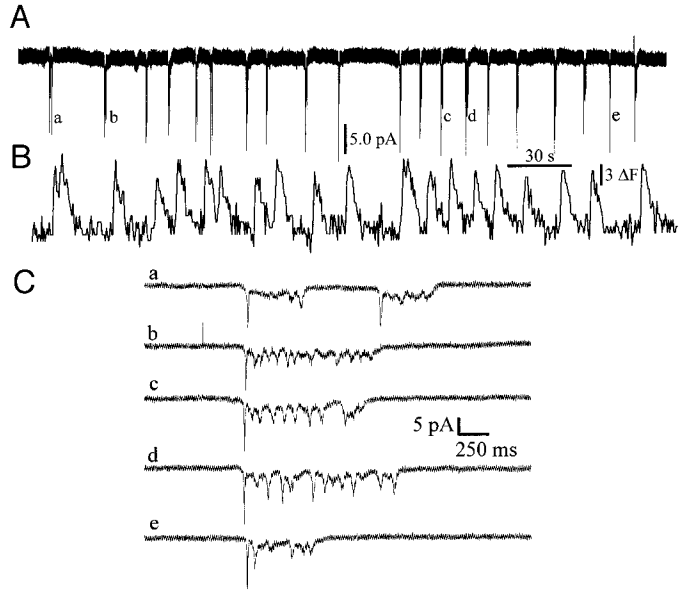

FIG. 1. Simultaneous measurement of action currents and Ca^{2+} oscillations. *A*: action currents measured in the cell-attached patch-clamp configuration. Currents are the electrical manifestation of action potentials when measured under these recording conditions. *B*: Ca^{2+} oscillations in an individual cell measured simultaneously with the action currents are aligned with respect to time. Note that the bursts of action currents precede each Ca^{2+} oscillation with a one-to-one relationship. An exception is 1 burst of action currents (e) that is not accompanied by a Ca^{2+} oscillation. *C*: individual bursts of action currents from *A* (*a–e*) are plotted with an expanded time scale to show the detail. Patch was voltage clamped to 0 mV with respect to the bath potential.

Groups of 5–50 cells within each field of 100–200 GT1–1 cells showed repetitive intercellular Ca^{2+} waves with consistent sites of initiation and patterns of propagation (Fig. 2). Ca^{2+} waves within an individual group were in some cases confined to that group, in some cases propagated to an adjoining group, and in some cases initiated by a wave originating in an adjoining group. GT1–1 cells appeared to have groups of cells that behaved as ''initiators'' and groups of cells (''followers'') that exhibited Ca^{2+} oscillations only as part of an intercellular wave propagated from neighboring cells. Action currents preceded the increase in $[Ca^{2+}]_i$ in all experiments regardless of whether the cell being measured was an initiator or a follower. The data in Fig. 1 are from a cell within a group of initiator cells, whereas the data in Fig. 2*C* are from a follower cell. The Ca^{2+} waves propagated to varying degrees away from the sites of initiation. An extensive wave is shown in Fig. 2*A* (*a–f*); the wave initiated in the *top right corner* of the field and propagated to the *left* and *down*, involving almost the entire field of cells. The position of the on-cell recording pipette is seen in a bright-field image (Fig. 2*B*). The acquisition time of each individual frame (*a–f*) is indicated on the tracing of measured electrical activity (Fig. 2*C*). Note that the burst of action currents occurs before the increase in $[Ca^{2+}]_i$ seen near the pipette. A more limited wave that initiated in the same group of cells but propagated to fewer cells is shown in Fig. 2*D*. The temporal pattern of the extensive and limited inter-

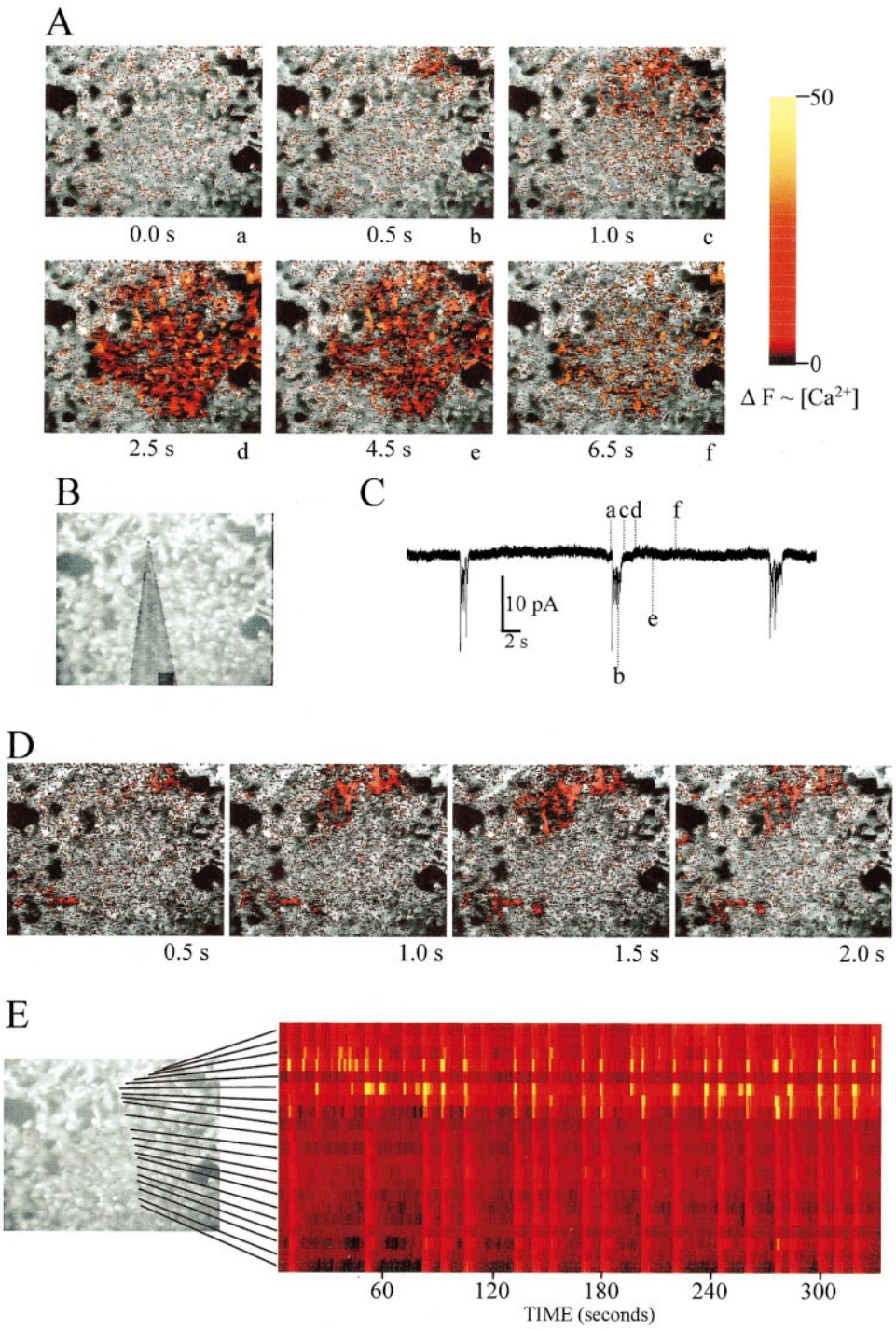

FIG. 2. Intercellular Ca^{2+} waves in GT1–1 neurons. *A*: wave of increased $[Ca^{2+}]_i$ is initiated (*top right*) and propagates to the *left* and *down* as shown (*a–f*). *B*: bright-field image of the position of the recording pipette in the field of cells. *C*: electrical waveform recorded in the cell-attached mode. Letters designate the frame numbers from *A*. Patch was voltage clamped to 0 mV with respect to the bath potential. *D*: smaller Ca^{2+} wave is initiated in the same group of cells but propagates to fewer cells. *E*: raster plot of Ca^{2+} increases from the same field of cells. Each row of the plot corresponds to the cell indicated (see text).

cellular waves was consistent throughout the 30-min recording. The limited waves occurred with a regular pattern having a mean interwave interval of 18 ± 0.25 (SE) s. The extensive waves appeared less frequently with an interwave interval of 24 ± 2 s. A raster plot from the same field of cells during a 5.5-min time period is shown in Fig. 2E. Each row of the plot corresponds to the cell indicated by the black line. Increases in $[Ca^{2+}]_i$ within individual cells are seen as bright bands within each row. The more extensive waves can be seen as bright vertical bands that traverse the entire plot while the more limited waves do not. The extensive waves appeared to cluster in groups of two to four waves separated by a longer time interval between clusters. Cells within sites of initiation and cells acting as followers were seen consistently in all experiments ($n = 39$).

The measured action currents in GT1–1 neurons could be due to voltage-gated Na^+ channels, Ca^{2+} channels, or both. Bath application of the potent voltage-gated Na^+ channel blocker TTX completely abolished the action currents (Fig. 3*A*; $n = 8$ cells) and Ca^{2+} waves (Fig. 3*B*; $n = 10$ coverslips). The L-type Ca^{2+} channel blocker nimodipine blocked the Ca^{2+} waves (Fig. 3*C*) but not the action currents (data not

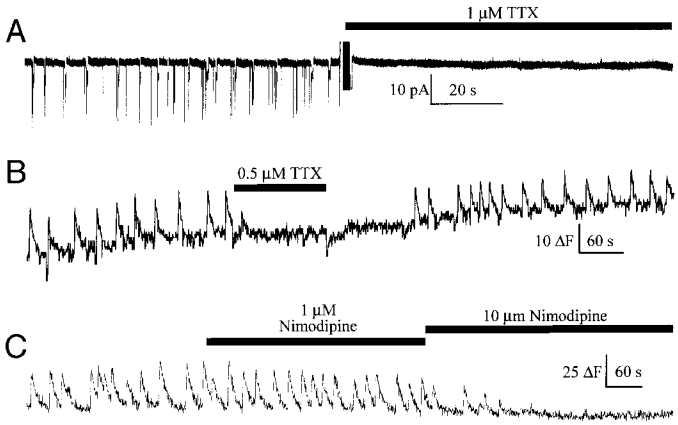

FIG. 3. Blockade of action currents and Ca^{2+} waves by tetrodotoxin (TTX). *A*: continuous recording of action currents. TTX is added to the bath where indicated by the bar. Patch was voltage clamped to 0 mV with respect to the bath potential. *B*: continuous recording of $[Ca^{2+}]_i$ from a different cell. TTX is present in the bath where indicated by the bar. *C*: Ca^{2+} oscillations were slowed and then blocked by 1 and 10 μM nimodipine, respectively.

shown; $n = 4$). The action currents did not require the influx of Ca^{2+}; they continued to fire after the removal of extracellular Ca^{2+} (Fig. 4*A; n* = 7 cells). Removal of extracellular Ca^{2+} caused a cessation in the Ca^{2+} waves that was reversible after a few minutes (Fig. 4*B; n* = 7 coverslips). These results indicate that the action currents are generated by Na^+ action potentials and that these action potentials are required to produce repetitive Ca^{2+} transients through the activation of voltage-gated Ca^{2+} channels.

The voltage-gated Ca^{2+} currents present in GT1–1 cells were characterized in terms of their sensitivity to voltage and Ca^{2+} channel toxins. Ca^{2+} channels are subdivided broadly based on the degree of depolarization required to open them. Low-voltage-activated (LVA) Ca^{2+} channels are opened by small depolarizations from the holding potential; high-voltage-activated (HVA) Ca^{2+} channels require depolarizations near −40 mV and above. HVA channels are subdivided further based on their sensitivity to peptide toxins and dihydropyridines (DHPs) (Birnbaumer et al. 1994). L-type HVA channels are blocked by DHP antagonists (such as nimodipine) and enhanced by DHP agonists. N-type HVA channels are blocked by the cone snail toxin ω-conotoxin GVIA (ω-CTx GVIA). P-type HVA channels are blocked by the funnel web spider toxin ω-agatoxin IVA (ω-Aga IVA). The currents through voltage-gated Ca^{2+} channels were measured in GT1–1 cells using Ba^{2+} as the charge carrier (Fig. 5). Currents elicited by voltage steps from the holding potential (−90 mV) to depolarized potentials are shown in Fig. 5*A*. The corresponding current-voltage (*I-V*) curve of peak inward currents is plotted (Fig. 5*B*). The *I-V* relationship is typical of HVA channels; the peak of the curve is near 10 mV and currents activate near −40 mV. There is an additional shoulder of current near −50 mV that may indicate that there is a component of LVA channels in these cells (Nowycky et al. 1985). The inward Ca^{2+} current was blocked completely by 200 μM Cd^{2+} (Fig. 5, *C* and *D*). The HVA current was not an N- or P-type current as the addition of ω-CTx GVIA or ω-Aga IVA had no effect on inward currents Fig. 5*C* ($n = 5$, both toxins). The time course of the blockade of peak currents by 200 μM Cd^{2+} as well as the lack of effect of N- and P-type channel blockers is shown in Fig. 5*D*. Nimodipine reduced the peak HVA currents by 0.70 ± 0.15 ($n = 6$) when compared with control currents (Fig. 5*E*). The time course of the current reduction by 50 μM nimodipine is shown in Fig. 5*F*. These results indicate that the HVA channels present in GT1–1 cells are predominantly L-type. There is, however, a residual component of HVA current that remains after the addition of nimodipine.

The measured cell-attached current waveform in GT1–1 cells consisted of at least two components; the Na^+ action currents and a sustained negative current of varied duration. The sustained current occurred near the end of a burst of action currents, and in some cases did not occur at all (Fig. 6). Action currents within a burst typically showed a progressively declining amplitude. Small spikes suggestive of truncated action currents (Figs. 1*C*, 6*A*, and 7) often were superimposed on the sustained negative current. Figure 6*A* shows three bursts of action currents with the sustained current, whereas a fourth burst had no sustained current. Recordings from two different cells (Fig. 6, *B* and *C*) illustrate further the temporal relationship between the two components as well as some of the variability seen in the duration of the sustained current.

The duration of action current bursts and the amplitude and duration of their accompanying sustained negative current were correlated with the amplitude and duration of Ca^{2+} transients (Fig. 7). Single action currents were often not associated with increases in $[Ca^{2+}]_i$. Longer trains of action currents with larger sustained negative currents were associated with longer and higher-amplitude Ca^{2+} transients.

Induction of action current firing in bovine chromaffin cells has been shown to occur with positive voltage pulses delivered to the pipette (Fenwick et al. 1982). The positive pulse in the pipette, while hyperpolarizing the patch itself, depolarizes the cell as a whole (to a lesser extent). A subset of GT1–1 cells (<10%) was capable of firing action currents in response to very small voltage pulses delivered to the pipette. A previously quiescent cell that fired action currents in response to small depolarizing pulses is shown in Fig. 8. An increase in the magnitude of the pulse delivered to the pipette caused an increase in the probability of action current firing (Fig. 8*A*) as well as a decrease in the latency to firing (Fig. 8*B*).

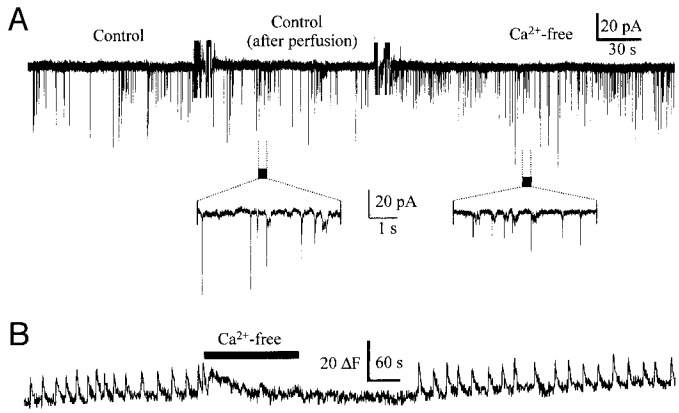

FIG. 4. Removal of extracellular Ca^{2+} abolishes the Ca^{2+} waves but not the action currents. *A*: continuous recording of action currents is plotted. Normal bath solution was perfused onto the cells and then a Ca^{2+}-free solution. *Insets*: expanded tracings. Patch was voltage clamped to 0 mV with respect to the bath potential. *B*: removal of extracellular Ca^{2+} reversibly inhibited the Ca^{2+} oscillations.

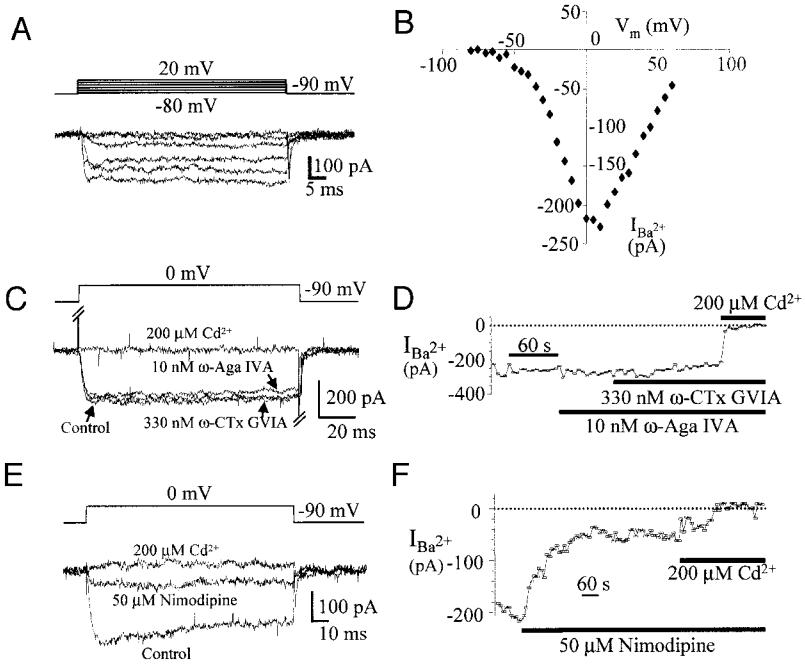

FIG. 5. High-voltage-activated (HVA) Ca^{2+} currents in GT1–1 cells are predominantly L-type. *A*: voltage pulse protocol and corresponding Ca^{2+} current sweeps used to construct the current-voltage curve shown in *B*. *C*: lack of an effect of P- and N-type channel blockers ω-agatoxin IVA (ω-Aga IVA) and [omega-conotoxin GVIA (ω-CTx GVIA) on whole cell HVA peak currents followed by a complete blockade caused by the addition 200 μM Cd^{2+}. *D*: time course of the blockade of HVA peak currents by Cd^{2+} and the lack of an effect of P- and N-type channel blockers. *E*: reduction of HVA peak currents by 50 μM nimodipine indicating that these channels are predominantly L type. *F*: time course of the current reduction by 50 μM nimodipine. Leak subtraction (P/N = −4) was used.

DISCUSSION

GT1–1 cells exhibit intrinsic activity characterized by spontaneous action potentials and increases in $[Ca^{2+}]_i$ that are either limited to individual cells or propagated to neighboring cells as an intercellular Ca^{2+} wave. The results presented here show that each increase in $[Ca^{2+}]_i$ in an individual cell is preceded by a burst of action potentials. The ionic mechanisms involved in the individual cell Ca^{2+} oscillations of GT1–7 and GT1–1 cells appear to be the same (Bosma 1993; Charles and Hales 1995). In both clones of the GT1 line, TTX blocks the action currents and the Ca^{2+} oscillations. Nimodipine or removal of extracellular Ca^{2+} eliminates the Ca^{2+} oscillations but not the spontaneous action currents. Ca^{2+} oscillations continue after depletion of intracellular stores with thapsigargin, and agents that cause Ca^{2+}-induced Ca^{2+} release have no effect on Ca^{2+} signaling (Charles and Hales 1995). These results are consistent with a model previously proposed in which a spontaneous membrane depolarization leads to the firing of Na^+-dependent action potentials, further cell depolarization, and an influx of Ca^{2+} through voltage-gated Ca^{2+} channels (Charles and Hales 1995).

The abolition of Ca^{2+} signaling by TTX shows that the firing of Na^+ -dependent action potentials is necessary for

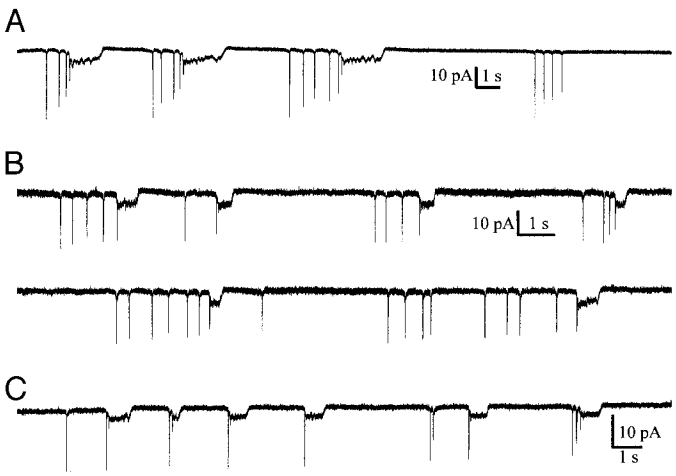

FIG. 6. Bursts of action potentials occur with variable patterns. *A*: continuous cell-attached recording showing 3 bursts of action currents each terminating with a sustained current. Fourth burst of action currents lacks the sustained current. *B*: continuous recording from a different cell showing action currents and the sustained current. *C*: continuous recording from a 3rd cell. In all of these cells, the patch was voltage clamped to 0 mV with respect to the bath potential.

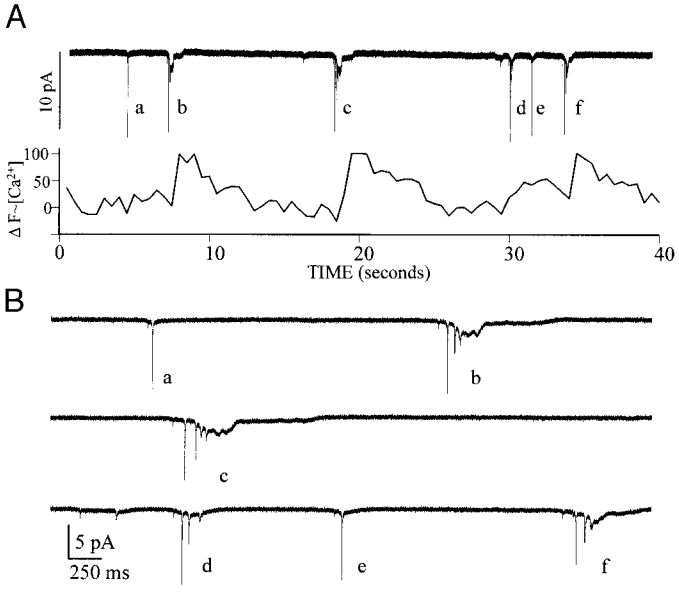

FIG. 7. Pattern of action current bursts is correlated with the pattern of Ca^{2+} oscillations. *A*: simultaneous recording from an individual cell. Tracings of the electrical activity and $[Ca^{2+}]_i$ are aligned with respect to time. Bursts of action currents are marked (a–f). *B*: action currents (a–f) displayed with an expanded time scale. Action current marked (a) that was not followed by a sustained current failed to initiate a Ca^{2+} increase. Burst marked (d) initiated a small increase in Ca^{2+}, whereas the bursts and sustained currents of (b, c, and f) initiated robust Ca^{2+} increases. Patch was voltage clamped to 0 mV with respect to the bath potential.

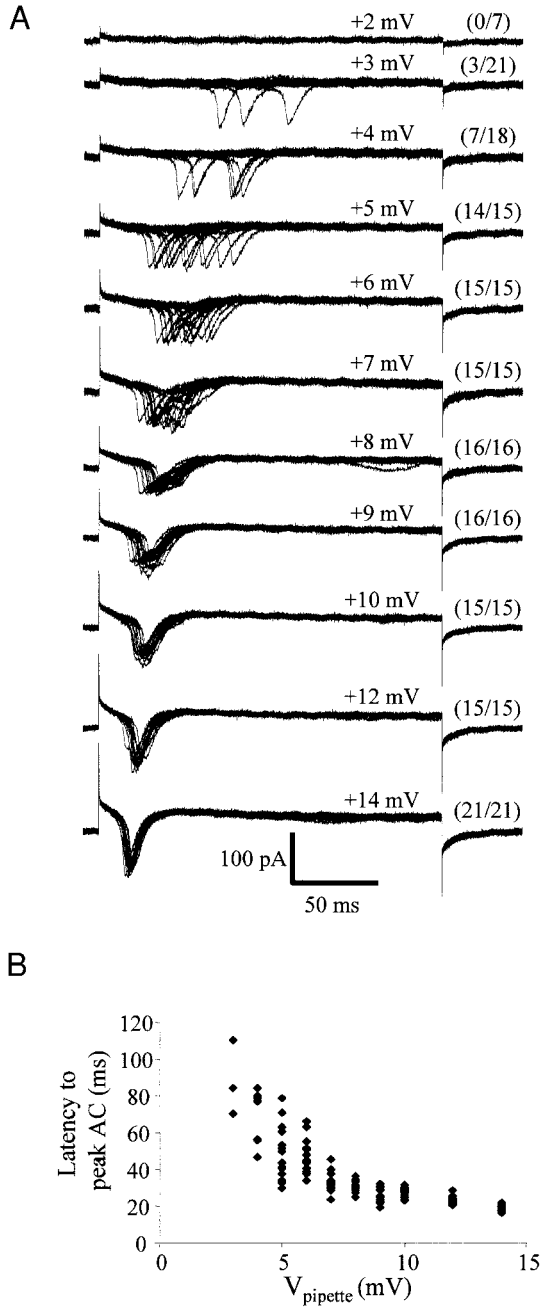

FIG. 8. Small pipette depolarizations lead to action potential firing in a previously quiescent cell. *A*: overlapping subsequent sweeps are plotted. Voltage step is delivered to the pipette to the voltage indicated above the sweeps. Patch is held at the bath potential (0 mV) between voltage steps. Delivery of a 2-mV step failed to initiate action current firing. Increasing the step to 3 mV caused a low probability (0.14) of action current firing that steeply increased to 0.39 and 0.93 by delivery of a 4- and 5-mV pulse, respectively. Voltage steps to ≥6 mV always resulted in the firing of an action current in this patch ($n = 113$). Numbers in parentheses are number of action currents fired/number of pulses delivered. *B*: latency to action current firing is plotted against the voltage step delivered to the pipette. Three-millivolt pulses elicited action currents with variable latencies >70 ms, whereas pulses to 14 mV consistently elicited action currents with latencies of ~20 ms.

Ca^{2+} oscillations to occur. This finding suggests that depolarizations of the membrane potential that underlie the spontaneous activity in GT1–1 neurons are not sufficient to cause influx of Ca^{2+} without the firing of Na^+ action potentials. A significant implication of this property is that the intercellular communication of a Ca^{2+} response requires the firing of action potentials in a neighboring cell, thereby creating a threshold for intercellular communication. Additionally, the finding that action potential bursts continue following the removal of extracellular Ca^{2+}, despite the abolition of all measurable Ca^{2+} signaling, indicates that the spontaneous electrical activity of GT1–1 cells does not require increases in $[Ca^{2+}]_i$.

GT1–1 cells differ from GT1–7 cells in that they are capable of Ca^{2+} signaling within groups of cells through coordinated intercellular Ca^{2+} waves. Our previous studies provide evidence that these intercellular Ca^{2+} waves are propagated through gap junctions composed of connexin26 (Charles et al. 1996). The results presented here are consistent with the hypothesis that the intercellular Ca^{2+} waves are mediated by a propagated depolarization rather than by the diffusion of Ca^{2+} itself. Ca^{2+} increases in individual cells always were preceded by action potentials—if the diffusion of Ca^{2+} was responsible for the propagation of the response, one would expect to see some increases in $[Ca^{2+}]_i$ that were not preceded by action potentials. This was never observed. The conclusion that the intercellular Ca^{2+} waves are propagated by depolarization also is supported by the observation that individual cells showed large increases in $[Ca^{2+}]_i$ that in some cases occurred as part of an intercellular wave and in some cases were limited to the individual cell.

The Ca^{2+} waves consistently originated from small groups of cells (initiators) and propagated through the field across cells acting as followers. The initiator cells were frequently near the edge of a field of cells or adjacent to a gap containing no cells. Otherwise there were no distinguishing morphological or electrophysiological characteristic of the cells that acted as initiators. These observations suggest that initiator cells do not represent a distinct subpopulation of cells but rather that they become initiators of intercellular activity because of their position in a field of cells and the amount of input they receive from neighboring cells.

The sustained negative current measured in the cell-attached configuration associated with a burst of action currents was correlated with the occurrence of a significant increase in $[Ca^{2+}]_i$ in that cell. At this time, we have not definitively identified the source of the current. The evidence that the sustained current occurs near the end of a burst of Na^+ spikes leads us to believe that it is activated when a cell becomes strongly depolarized. There are at least two possible explanations for this current. The first possibility is that the current is due to outward ionic currents passing through voltage-activated K^+ channels in the patch of membrane that is delimited by the pipette. A second possibility is that the sustained current is due to a decrease in the resistance of the cell membrane due to the opening of voltage-gated Ca^{2+} and K^+ channels that cause a short-circuiting of the membrane and a deformation of the action current waveform.

The small depolarizing stimulus required to evoke the firing of action potentials indicates that GT1–1 cells have a resting potential that is close to the threshold for action potentials (Fig. 8). In addition, the latency to firing and the probability of action potential firing depends on the strength of the depolarizing input. Because each GT1–1 cell receives input from multiple neighboring cells, different patterns of action potential bursts may result from the integration of these multiple inputs.

Different patterns of action potential bursts evoke Ca^{2+} signals with different amplitudes and durations as shown in Fig. 7. Differences in the patterns of Ca^{2+} signaling may be important for changes to Ca^{2+}-dependent GnRH release by individual cells.

GT-1 cells have been shown to possess the features of the GnRH pulse generator: namely rhythmic, pulsatile release of GnRH with a frequency similar to that measured in rodents (Kawakami et al. 1982; Martinez de la Escalera et al. 1992). At this stage, it is not clear how the patterns of electrical and Ca^{2+} signaling in GT1–1 cells are related to a pulsatile pattern of GnRH release. Pulsatile release could be stimulated by a change in the frequency of spontaneous signaling, a change in cellular coupling, a change in secretory function, or some combination of the above. We are presently pursuing simultaneous measurement of GnRH secretion by GT1–1 cells to identify patterns of electrical and Ca^{2+} signaling that are correlated with pulsatile GnRH release.

This work was supported by National Institute of Neurological Disorders and Stroke Grants R29-NS-32283 and P01-NS-02808 to A. C. Charles.

Address reprint requests to J. L. Costantin.

Received 29 December 1998; accepted in final form 23 March 1999.

REFERENCES

BEZANILLA, F. AND ARMSTRONG, C. M. Inactivation of the sodium channel. I. Sodium current experiments. *J. Gen. Physiol.* 70: 549–566, 1977.

BIRNBAUMER, L., CAMPBELL, K. P., CATTERALL, W. A., HARPOLD, M. M., HOFMANN, F., HORNE, W. A., MORI, Y., SCHWARTZ, A., SNUTCH, T. P., TANABE, T., AND TSIEN, R. W. The naming of voltage-gated calcium channels. *Neuron* 13: 505–506, 1994.

BOSMA, M. M. Ion channel properties and episodic activity in isolated immortalized gonadotropin-releasing hormone (GnRH) neurons. *J. Membr. Biol.* 136: 85–96, 1993.

BOURGUIGNON, J. P., GERARD, A., ALVAREZ GONZALEZ, M. L., AND FRANCHIMONT, P. Control of pulsatile secretion of gonadotrophin releasing hormone from hypothalamic explants. *Hum. Reprod.* 8, *Suppl.* 2: 18–22, 1993.

CARDENAS, H., ORDÈOG, T., O'BYRNE, K. T., AND KNOBIL, E. Single unit components of the hypothalamic multiunit electrical activity associated with the central signal generator that directs the pulsatile secretion of gonadotropic hormones. *Proc. Natl. Acad. Sci. USA* 90: 9630–9634, 1993.

CHARLES, A. C. AND HALES, T. G. Mechanisms of spontaneous calcium oscillations and action potentials in immortalized hypothalamic (GT1–7) neurons. *J. Neurophysiol.* 73: 56–64, 1995.

CHARLES, A. C., KODALI, S. K., AND TYNDALE, R. F. Intercellular calcium waves in neurons. *Mol. Cell. Neurosci.* 7: 337–353, 1996.

CHARLES, A. C., MERRILL, J. E., DIRKSEN, E. R., AND SANDERSON, M. J. Intercellular signaling in glial cells: calcium waves and oscillations in response to mechanical stimulation and glutamate. *Neuron* 6: 983–992, 1991.

CLARKE, I. J. AND CUMMINS, J. T. The temporal relationship between gonadotropin releasing hormone (GnRH) and luteinizing hormone (LH) secretion in ovariectomized ewes. *Endocrinology* 111: 1737–1739, 1982.

FENWICK, E. M., MARTY, A., AND NEHER, E. A patch-clamp study of bovine chromaffin cells and of their sensitivity to acetylcholine. *J. Physiol. (Lond.)* 331: 577–597, 1982.

HALES, T. G., SANDERSON, M. J., AND CHARLES, A. C. GABA has excitatory actions on GnRH-secreting immortalized hypothalamic (GT1–7) neurons. *Neuroendocrinology* 59: 297–308, 1994.

HAMILL, O. P., MARTY, A., NEHER, E., SAKMANN, B., AND SIGWORTH, F. J. Improved patch-clamp techniques for high-resolution current recording from cells and cell-free membrane patches. *Pflügers Arch.* 391: 85–100, 1981.

KAWAKAMI, M., UEMURA, T., AND HAYASHI, R. Electrophysiological correlates of pulsatile gonadotropin release in rats. *Neuroendocrinology* 35: 63–67, 1982.

KNOBIL, E. The neuroendocrine control of the menstrual cycle. *Recent Prog. Horm. Res.* 36: 53–88, 1980.

KNOBIL, E. The hypothalamic gonadotrophic hormone releasing hormone (GnRH) pulse generator in the rhesus monkey and its neuroendocrine control. *Hum. Reprod.* 3: 29–31, 1988.

KRSMANOVIC, L. Z., STOJILKOVIC, S. S., MERELLI, F., DUFOUR, S. M., VIRMANI, M. A., AND CATT, K. J. Calcium signaling and episodic secretion of gonadotropin-releasing hormone in hypothalamic neurons. *Proc. Natl. Acad. Sci. USA* 89: 8462–8466, 1992.

MARTINEZ DE LA ESCALERA, G., CHOI, A. L., AND WEINER, R. I. Generation and synchronization of gonadotropin-releasing hormone (GnRH) pulses: intrinsic properties of the GT1–1 GnRH neuronal cell line. *Proc. Natl. Acad. Sci. USA* 89: 1852–1855, 1992.

MELLON, P. L., WINDLE, J. J., GOLDSMITH, P. C., PADULA, C. A., ROBERTS, J. L., AND WEINER, R. I. Immortalization of hypothalamic GnRH neurons by genetically targeted tumorigenesis. *Neuron* 5: 1–10, 1990.

MORI, Y., NISHIHARA, M., TANAKA, T., SHIMIZU, T., YAMAGUCHI, M., TAKEUCHI, Y., AND HOSHINO, K. Chronic recording of electrophysiological manifestation of the hypothalamic gonadotropin-releasing hormone pulse generator activity in the goat. *Neuroendocrinology* 53: 392–395, 1991.

NOWYCKY, M. C., FOX, A. P., AND TSIEN, R. W. Three types of neuronal calcium channel with different calcium agonist sensitivity. *Nature* 316: 440–443, 1985.

PETERS, J. A., LAMBERT, J. J., AND COTTRELL, G. A. An electrophysiological investigation of the characteristics and function of GABAA receptors on bovine adrenomedullary chromaffin cells. *Pflügers Arch.* 415: 95–103, 1989.

WETSEL, W. C. Immortalized hypothalamic luteinizing hormone-releasing hormone (LHRH) neurons: a new tool for dissecting the molecular and cellular basis of LHRH physiology. *Cell. Mol. Neurobiol.* 15: 43–78, 1995.

WETSEL, W. C., VALENĞCA, M. M., MERCHENTHALER, I., LIPOSITS, Z., LÂOPEZ, F. J., WEINER, R. I., MELLON, P. L., AND NEGRO-VILAR, A. Intrinsic pulsatile secretory activity of immortalized luteinizing hormone-releasing hormone-secreting neurons. *Proc. Natl. Acad. Sci. USA* 89: 4149–4153, 1992.

WILSON, R. C., KESNER, J. S., KAUFMAN, J. M., UEMURA, T., AKEMA, T., AND KNOBIL, E. Central electrophysiologic correlates of pulsatile luteinizing hormone secretion in the rhesus monkey. *Neuroendocrinology* 39: 256–260, 1984.